HIGH RESOLUTION IMAGING OF THE OCEAN SURFACE BACKSCATTER BY INVERSION OF ALTIMETER WAVEFORMS

J. Tournadre, B. Chapron, N. Reul, Y. Quilfen

IFREMER, Laboratoire d'Océanographie Spatiale
Plouzané, France

1. INTRODUCTION

All the satellite altimeters use pulse-limited-geometry and full-deramp technique to measure the power backscatter by the ocean surface as a function of time, i.e. the altimeter pulse echo waveform, see for example [1] for explanation on pulse limited altimeters). Assuming that the distribution of the sea surface roughness and elevation are homogeneous over the altimeter footprint, the backscatter coefficient of the echo waveform can be expressed as a double convolution product of the radar point target response, the flat sea surface response and the joint probability density function of slope and elevation of the sea surface [2, 3]. Further assuming a Gaussian shape for the antenna beam pattern, the compressed altimeter pulse P and the joint probability of sea surface slope and elevation, the cross section as a function of time follows the classical Brown (1977) model. However, previous studies such as [4, 5] have shown that the basic assumption of the Brown model, the homogeneity of the sea surface roughness distribution is not always valid. In particular in presence of rain, sea ice,small island or reef, surface slick or under very low wind conditions.

In such cases, an altimeter can be seen as an imager of the sea surface backscatter whose imaging process is more complex than a classical one in the sense that pixels are not rectangular but annular. We present a method to invert the measured waveforms in terms of surface backscatter at a resolution of the order of the along track 20 Hz resolution (290 m for JASON). The method is then validated using simulated waveforms and is shown to be unbiased and to have an rms of the order of 0.25 dB. Several applications concerning surface slicks, small islands and submerged reefs, interaction between current and backscatter are presented.

2. ALTIMETRY PRINCIPLE

Figure 2 shows an altimeter pulse being reflected from a flat surface. As the pulse advances, the illuminated area grows rapidly from a point to a disk, as does the returned power. Eventually, an annulus is formed and the geometry is such that the annulus area remains constant as the diameter increases. The returned signal strength, which depends on the reflecting area, grows rapidly until the annulus is formed, remains constant until the growing annulus reaches the edge of the radar beam, where it starts to diminish. Assuming a Gaussian shape of standard deviation u_b for the antenna beam pattern, a Gaussian shape of standard deviation σ_τ for the compressed altimeter pulse and also a Gaussian joint probability of sea surface slope and elevation, under the small angle approximation, the cross section σ simplifies to the classical Brown model

$$\sigma(t) = \frac{1}{2}(2\pi)^{3/2} H'' \sigma_\tau \sigma_0 \left(1 + \mathtt{erf}\left(\frac{ct/2}{\sqrt{2}\sigma_p}\right)\right) e^{-\frac{ct/2}{u_b}} \tag{1}$$

where erf is the error function, σ_0 is the surface backscatter, H'' is the extended satellite height, σ_p is defined by $\sigma_p = \sqrt{h^2 + \sigma_\tau^2}$; h being the rms wave height.

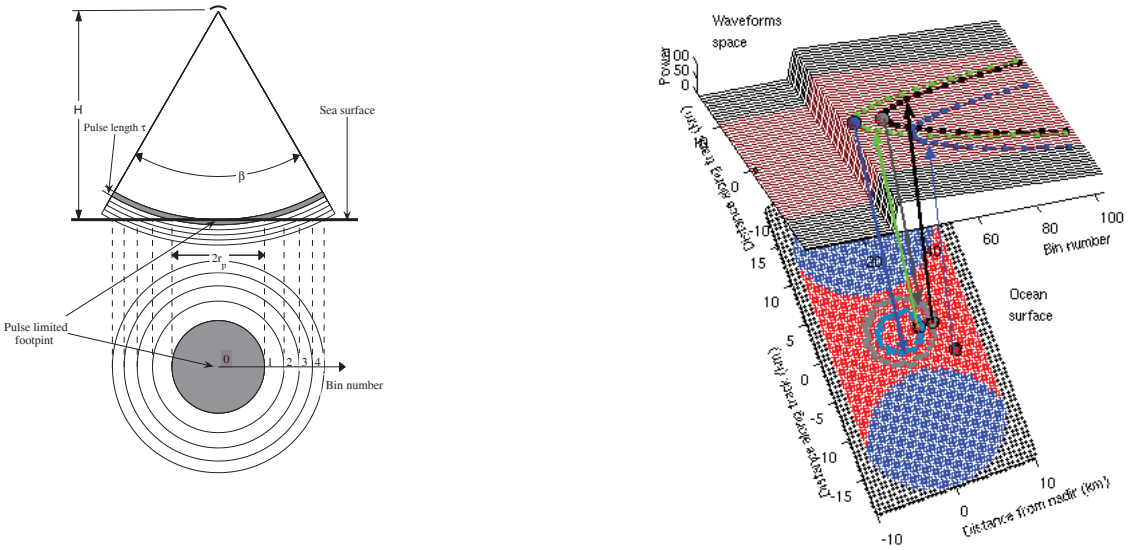

(a) (b)

Fig. 1. Geometry of the altimeter ocean surface sampling (a) and schematic representation of the altimeter ocean surface imaging process.

When the surface backscatter strongly varies at scales smaller than the altimeter footprint diameter, the waveform can significantly differ from the Brown model. The altimeter can be seen as an imager of the sea surface backscatter whose imaging process is more complex than the classical ones in the sense that pixels are annular (see figure 2). The measured backscatter as a function of time can be, in a first order approximation, expressed as

$$\sigma_0(t) = \alpha \int_0^{2\pi} \int_0^{\infty} \sigma_s(u,\theta) e^{-\frac{u}{u_b}} e^{-\frac{(ct/2-u)^2}{2\sigma_p^2}} du d\theta \tag{2}$$

where $\alpha = \frac{\pi^2 H'' |R(0)|^2 \sigma_\tau}{2\sigma_p}$ is a normalization coefficient, θ is the azimuth, u is the range and σ_s is the surface backscatter.

3. INVERSION OF THE ALTIMETER WAVEFORMS

The altimeter measured waveforms are given in telemetry samples of width τ (length of the pulse) and the nominal track point (i.e. the sea level or $t = 0$) is shifted to bin 32.5. Assuming that the surface backscatter is defined on a regular along track grid, and further assuming that the rms of the surface is small (low wave height), equation 2 can be discretized as follow, the j^{th} element of the i^{th} waveform ($w_f(i,j)$) is the summation of surface backscatter ($\sigma_s(k,l)$) that corresponds to the same gate range u_j, i.e.

$$w_f(i,j) = \alpha \sum_k \sum_l \sigma_s(k,l) e^{-\frac{u(k,l)}{u_b}} (1 + erf(\frac{u_j}{\sqrt{2}\sigma_p})) \tag{3}$$

where the range of k and l verifies

$$u(k,l) = \frac{(x_{kl} - x_i^0)^2 + (y_{kl} - y_i^0)^2}{H'' c\tau} = u_j \tag{4}$$

where x and y are the along and across track coordinates and x_i^0 and y^0 are the nadir coordinates corresponding to the i^{th} waveform. As u_j is constant, equation 4 simplifies to

$$W(i,j) = w_f(i,j)\frac{e^{\frac{u_j}{u_b}}}{(1+erf(\frac{u_j}{\sqrt{2}\sigma_p}))} = \alpha \sum_k \sum_l \sigma_s(k,l) \tag{5}$$

where W represents the waveform detrended for the beam-width and wave height effects.

As it can be seen in figure 2, an element of the surface has a parabolic image in the waveform space which itself has a circular image in the surface space. It should be noted that because of the altimeter sampling geometry two symmetrical points with respect to the x (along track) axis have identical images so that there is a left/right ambiguity. If we consider a series of waveform W_i, $i = 1..N$ (in red in the figure), they constitute the image of the ensemble of blue points of the surface. The waveforms (detrended for the beam-width and wave height effects) can be written in matrix form as

$$W = AS \tag{6}$$

where A is an imaging matrix that depends only of the altimeter geometry and can be easily computed. It is a 5400 by 3400 matrix defining an overdetermined system. It is thus possible to compute a pseudo Moore-Penrose inverse A^+ using singular value decomposition [6] and thus to invert equation 6, as said before there exists a left/right ambiguity so it is only possible to estimate the mean value of the symmetrical points.

$$S = A^+W \tag{7}$$

It should be noted that within the ensemble of surface elements only the central ones (in red in figure 2) have images that are completely included in the selected waveforms. Only those are considered during the inversion process.

4. VALIDATION

The method has first been tested using a constant surface backscatter and noisy (white noise of 0.25 dB rms) surface backscatter. The waveforms are computed using the Brown model and are then inverted using equation 7. The bias is smaller than 0.02 dB and the rms smaller than 0.05 dB for the constant case. This show that the inversion is unbiased and has a very good precision. For the noisy case, the bias is smaller than 0.05 dB and the rms is of the same order as the surface backscatter rms. It should be noted that because of the sampling geometry the rms is larger near the nadir.

5. EXAMPLE OF APPLICATION

Several applications of the method can be foreseen and an operational high resolution backscatter altimeter product could be defined. Among the applications, figure 5 presents an example of the analysis of a sigma-bloom event ([7]) near Indonesia. The waveforms (fig 5-a) exhibit the classical parabolic patterns associated to strong surface backscatter variations These patterns are associated to small surface patches of very high backscatter corresponding to either very calm zone (such as the ones observed on SAR imagery [8] or surface films. The inverted σ_0 field allows a precise estimation of the area of the very backscatter and could help to better understand the air-sea interactions. Other applications concern the analysis of the impact of surface current on the surface backscatter, the detection of small island, the effect of submerged reef, the analysis of the land/sea transition or the study of the amazon river flooding.

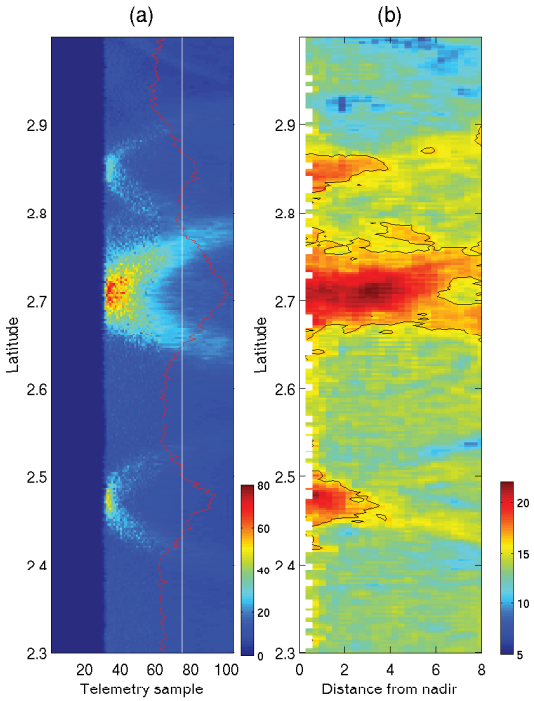

Fig. 2. Example of inversion of Envisat altimeter waveforms during a sigma-bloom event. (a) measured waveforms, the red line presents the measured 18Hz backscatter (x4), (b) inverted surface backscatter in dB, the 20 dB isoline is shown as a black line.

6. REFERENCES

[1] Dudley B. Chelton, Edward J. Walsh, and John L. MacArthur, "Pulse Compression and Sea Level Tracking in Satellite Altimetry," *Journal of Atmospheric and Oceanic Technology*, vol. 6, no. 3, pp. 407–438, 1989.

[2] G. S. Brown, "The average impulse response of a rough surface and its applications," *IEEE Trans. Antennas Propag.*, vol. AP-25, pp. 67–74, 1977.

[3] D.E. Barrick and B.J. Lipa, "Analysis and interpretation of altimeter sea echo," *Satellite Oceanic Remote Sensing, Advances in Geophysics*, vol. 27, pp. 61–100, 1985.

[4] J. Tournadre, "Determination of rain cell characteristics from the analysis of Topex altimeter echo waveforms," *J. Atmos. Oceanic Technol.*, vol. 15, no. 2, pp. 387–406, Apr. 1998.

[5] J. Tournadre, B. Chapron, N. Reul, and D. C. Vandemark, "A satellite altimeter model for ocean slick detection," *J. Geophys. Res.*, vol. 111, no. C4, pp. C04004, Apr. 2006.

[6] R. Penrose, "A generalized inverse for matrices," *Proceedings of the Cambridge Philosophical Society*, vol. 51, pp. 406–413, 1955.

[7] G.T. Mitchum, D.W. Hancock, G.S. Hayne, and D.C. Vandemark, "Blooms of sigma0 in the TOPEX radar altimeter data," *J. Atmos. Oeanic Tech.*, vol. 21, pp. 1232–1245, 2004.

[8] P. Clemente-Colón and X.-H. Yan, "Low backscatter features in SAR imagery," *JHU/APL Tech. Digest*, vol. Vol. 21, no. 1, pp. 116–121., 2000.